RF OPERATION EXPERIENCE AT THE EUROPEAN XFEL

J. Branlard[†], V. Ayvazyan, Ł. Butkowski, M. Grecki, M. Hierholzer, Mar. Hoffmann,
Mat. Hoffmann, M. Killenberg, D. Kostin, T. Lamb, L. Lilje, U. Mavrič, M. Omet, S. Pfeiffer,
R. Rybaniec, H. Schlarb, C. Schmidt, N. Shehzad, V. Vogel, N. Walker, DESY, Hamburg, Germany

Abstract

After its successful commissioning during the first half of 2017, the European X-ray free electron laser is now in regular operation delivering photons to users since September 2017.

This contribution presents an overview on the experience gathered during the first couple of years of operation. In particular, the focus is set on RF operation, advanced commissioning and RF related machine studies.

INTRODUCTION

The European X-ray free electron laser (XFEL) is a user facility delivering ultra-short hard and soft X-ray flashes with the highest brilliance worldwide, through 3 undulator lines and serving up to 6 experiments. It is based on a 10 Hz pulsed 17.5 GeV superconducting linac, commissioned since 2017. The first self-amplified spontaneous emission (SASE) light was demonstrated in May 2017, the first user run took place in September 2017 delivering photons at a wavelength of 1.3 Å. After a month shutdown in April 2018, the last 2 RF stations were commissioned. In May 2018, lasing was demonstrated simultaneously in all 3 beam lines (SASE 1, 2 and 3). A total of 1600 hours are devoted to user programs in 2018; this number should increase to 4800 hours in 2019. A summary on the machine commissioning and its highlights is given in [1, 2]. In this contribution, the focus is set on the experience gathered during the first operation years of the XFEL, in particular the commissioning of the LLRF system beyond its basic functionality, reported in the following section and an insight on a couple of dedicated machine studies is given in the subsequent section.

LLRF ADVANCED COMMISSIONING

The LLRF commissioning procedure was first presented in [3], and the accelerator operation and performance was reported in [4]. These commissioning steps guaranteed the proper operation of all RF stations, controlling the RF field inside the superconducting cavities and accelerating the beam to the desired energy. The advanced LLRF commissioning covers taking into operation LLRF subsystems related to performance optimization such as the drift compensation module [4], or modules related to more advanced exception handling mechanism such as the klystron lifetime management system (KLM) [5]. Figure 1 gives an example of this protection mechanism where a sudden increase in reflected power (P_{REFL}) was observed on one arm of the 10 MW klystron. This anomaly was detected within 200 nsec and resulted in switching

off the drive 600 nsec later, preventing a high reflected waveform potentially harmful for the klystron. The increase in P_{REFL} is likely due to waveguide sparking, which started appearing when operating the klystron above 7 MW.
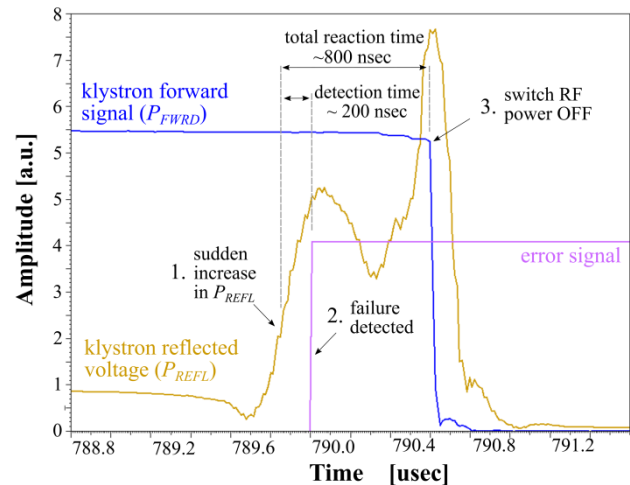

Figure 1: Event observed on August 29th 2018 at station A6. A sudden increase of the reflected power (1) triggered the klystron management system (2) to stop the klystron drive (3).

During this advanced commissioning phase, servers to monitor and service LLRF auxiliary modules were also deployed and commissioned (modules responsible for the local oscillator and clock generation, for the power supplies, for the remote controllable fuse and relay submodules or for the piezo driver for example). During this phase, firmware and server updates were deployed to improve the performance of the LLRF system. One can cite the toroid-based beam loading compensation algorithm as an example [6]. The optical RF synchronization (REFM-OPT) module was also taken into operation. This module synchronizes the 1.3 GHz RF reference distributed along the accelerator with respect to sub-fs stabilised optical links. Based on a Mach-Zender modulator, the REFM-OPT compares the phases of the optical link and RF signals and corrects for any drifts taking place in the RF distribution chain [7]. The re-synchronized RF is distributed locally to the nearest RF stations. The plot in Fig. 2 shows the temperature drift measured in the Linacs 1, 2 and 3 and the corresponding phase corrections applied by the different REFM-OPT units along the accelerator. Although there were no temperature data available for the injector, the tighter ambient temperature regulation in the injector directly translates into smaller reference phase corrections required from the injector REFM-OPT.
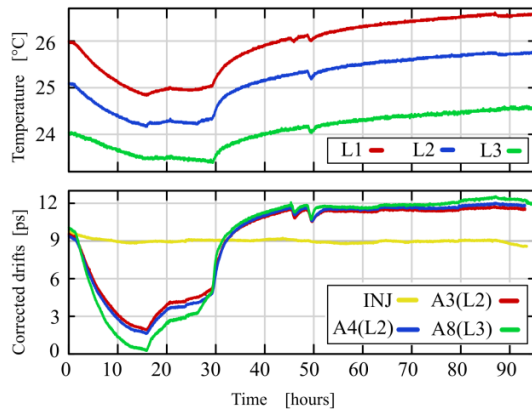
Figure 2: Temperature drifts measured in the different sections of the main accelerator, and the reference phase corrections applied by the REFM-OPTs.

RF SPECIFIC OPERATION STUDIES

Energy Reach and Radiation Related Studies

Since last year, weekly studies are devoted to assess the maximum reachable gradient for individual RF stations [4]: the possible limiting factors being (1) cavity quench, (2) field emission or (3) limitations coming from the high power chain (modulator voltage, waveguide sparks…). The RF station is time shifted off beam so that the investigation can take place parasitically along normal machine operation and beam delivery. Special care is taken to fine tune the cavity coupling, to verify the calibration of forward and reflected power with respect to probe signals, and to tune all cavities for all investigated gradient set points. Gradient limiters and quench reaction algorithms are disabled; finally, the beam block mechanism triggered by the machine protection system is masked for this station. This measure guarantees that quenching the station under investigation does not inhibit beam transport. The gradient is then carefully increased in open loop until one the 3 limitations mentioned above is encountered.

Although sometimes operating in full saturation, insufficient klystron power is most often not the limiting factor; a waveguide spark, quench or field emission is. Quenches are detected by the quench detection system, while field emission is measured by the online radiation monitor, the dark current monitor and periodic runs of the radiation measurement robot [8]. In the example of Fig. 3, the gradient of station A12 was increased, triggering a field emitter in one of the cavities. The resulting increase in radiation scattered to the nearest stations upstream (A11) and downstream (A13) was measured with thermoluminescent dosimeters (TLDs) placed underneath the cryomodules. The control electronics is protected by a concrete shielding, damping the radiation by a factor of 20-30. Nevertheless, the higher rate of 60 mGy/day observed outside the shielding of A12 was evaluated to be too high for the acceptable threshold of 1 Gy per year for the electronics underneath the concrete shielding. The operating gradient of A12 was subsequently reduced. For

the weekly scans performed by the radiation monitor robot, an administrative limit of 500 μSv/h was set, which was reached on a couple of stations so far (A9 and A12).
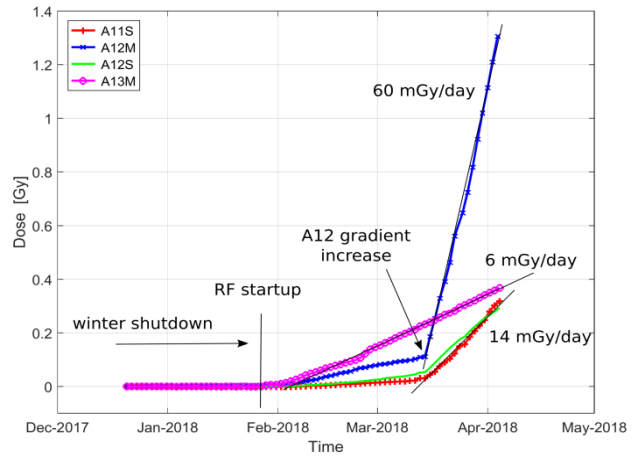

Figure 3: Accumulated radiation dose measured by TLDs placed underneath the cryomodules and outside the electronic shielding (M and S are the master and slave LLRF).

In the case where the limiting factor is a quench, the limiting cavity is detuned and the energy set point ramp up is repeated. In some cases, detuning the limiting cavity(-ies) might still result in a higher overall energy gain for the RF station. This can be mostly explained by the fact that the tailoring of the waveguide distribution according to each cavity performance has inherent limitations and limited precision. Removing the weakest cavity (by detuning it) can at times facilitate achieving maximum performance out of other cavities, yielding a net energy gain. 16 cavities (2%) fell in that category and were detuned as a consequence.
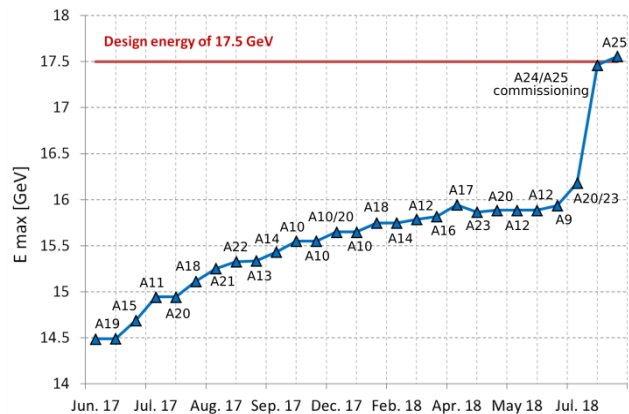

Figure 4: incremental energy gain resulting from the maximum gradient investigations (delta markers).

The outcome of each investigation is a report summarizing the findings and possibly proposing an optimization scenario. The energy gain observed since the beginning of this energy reach campaign is illustrated in Fig. 4. The steady raise comes from investigation of individual RF stations. The large step in July 2018 corresponds to the

commissioning of the last 2 RF stations (A24 and A25) for which the installation was finalized during the April shutdown. The milestone of reaching the XFEL design energy of 17.5 GeV was then achieved mid of July 2018.

Cryogenic Pressure versus Detuning Study

Another study was carried out to evaluate the dependency of cavity detuning on fluctuations of the cryogenic helium (He) pressure (see Fig. 5). In this study, the He pressure was purposefully changed by ±3 mBar from its nominal 30 mBar set point over a total of 8 hours, while measuring the detuning for all 1.3 and 3.9 GHz cavities in the accelerator. The RF was kept constant for all RF stations, operating in open loop at a reduced gradient (typ. 10 MV/m per cavity) to minimize the impact of Lorentz force detuning and reduce the risk of high-power related RF trips. The outcome is a detuning sensitivity of 39.6 ±3 Hz/mBar for the 1.3 GHz cavities and 62.4 ±2 Hz/mBar for the 3.9 GHz cavities, in good agreement with the partial measurement reported in [9].
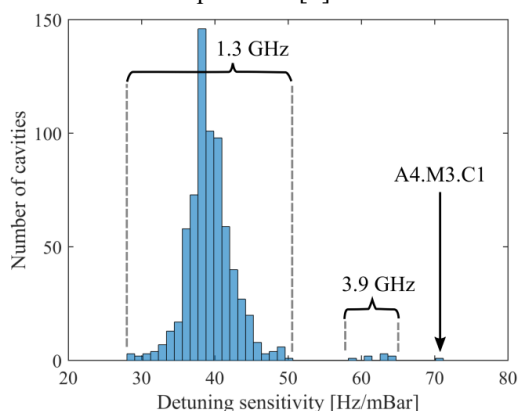

Figure 5: Histogram of the detuning sensitivity to He pressure fluctuations for XFEL superconducting cavities.

In the absence of piezo resonance control and for the XFEL cavity half bandwidth of 140 Hz, the typical 20% RF power overhead reserved for controls would be consumed compensating for a detuning of ±130 Hz. This corresponds to ±3.28 mBar He pressure fluctuation for the measured 1.3 GHz sensitivity. A ±3 mBar safety threshold was then set on the He pressure, beyond which RF operation is not allowed. The typical He pressure stability is better than 0.1 mBar rms, so this interlock system would prevent operation, should an uncontrolled drift of the He pressure occur. Although the sensitivity of the third harmonic cavities is higher, the situation there is relaxed due to their broader bandwidth. It is worth mentioning the special case of the first cavity, in the third cryomodule of the fourth RF station (A4.M3.C1) whose sensitivity is almost twice as high as the average 1.3 GHz cavities. This peculiarity had been caught during the cryomodule horizontal tests, but does not hinder regular operation. As a final remark, we have also observed some hysteresis effect accounting for ~50 Hz on 8 cavities (~1%). These cavities did not return to their initial tuning and required retuning although the initial He pressure had been re-

stored. In almost all cases, this was observed on the first cavity of a cryomodule. This hysteresis effect is not yet fully understood. One explanation could be linked to the fact that the first half cell of the first cavity in a cryomodule is not included in the He vessel and therefore exhibits a slightly different cooling profile.

CONCLUSION

This contribution gives an overview on the continued RF commissioning and RF related studies performed at the European XFEL. In particular, some aspects of the advanced LLRF commissioning such as klystron lifetime management and optical reference synchronization were described. An insight on some RF operation related studies was also presented to illustrate the continuing work to better understand and characterize this new accelerator. Two examples were given, one illustrating the effort to assess the maximum gradient the European XFEL can reach and the limiting factors; another to assess the dependency of cavity detuning on the stability of the cryogenic He pressure. While the focus will shift in the coming years towards more user operation and less machine study time, the XFEL operation team is building up the effort to increase machine availability and reliability. This includes developing tools to catch, analyze and document any RF trips, their root cause and recovery time. More sophisticated tools to help operators monitor the health of the LLRF systems and the machine in general or tools to automate system start up, calibration procedures and optimize performance are also under development.

REFERENCES

[1] M. Scholz et al., "FEL performance achieved at European XFEL", Proc. of IPAC'18, Vancouver, Canada, May 2018.

[2] D. Noelle et al., "Commissioning of the European XFEL", Presented at LINAC'18, Beijing, China, Sept. 2018.

[3] J. Branlard et al., "Installation and first commissioning of the LLRF system for the European XFEL", Proc. of IPAC'17, Copenhagen, Denmark, May 2017.

[4] M. Omet et al., "LLRF operation and performance at the European XFEL", Proc. of IPAC'18, Vancouver, Canada, May 2018.

[5] Ł. Butkowski et al., "A Model-Based Fast Protection System for High-Power RF Tube Amplifiers Used at the European XFEL Accelerator", IEEE Trans. on Nuclear Science, vol. 64, no. 6, Jun. 2017.

[6] Ł. Butkowski et al., "Implementation of the Beam Loading Compensation Algorithm in the LLRF System of the European XFEL ", presented at LINAC18, Beijing, China, Sept. 2018.

[7] T. Lamb, et al. "Laser-to-RF synchronization with femto-second precision", Proc. of FEL'17, Santa Fe, NM, USA, Aug. 2017.

[8] A. Dehne et al., "MARWIN: a mobile autonomous robot for maintenance and inspection", Proc. of ICALEPCS'17, Barcelona, Spain, Oct. 2017.

[9] R. Paparella et al. "Operational Experience of the European-XFEL 3.9 GHz Coaxial Tuners", Proc. of SRF'17, Lanzhou, China, Aug. 2017.

Electron Accelerators and Applications

FELs